Dietrich Grauerholz was born in Krems II, Germany, on September 22, 1945. He received the Dipl.-Ing. in 1971.

From 1971 to 1973 he worked in the High-Frequency Laboratory of Elektro-Spezial (Philips). In 1973 he joined the Microwave Department of the University of Bremen, where he has been engaged in the research and development of microstrip circuits, fin-line structures, and microwave measurements.

Rüdiger Vahldieck was born in Heiligenhafen, Germany, on July 8, 1951. He received his Dipl.-Ing. degree in electrical engineering from the University of Bremen, West Germany, in 1980.

His present research activities are in the field of microwave integrated circuits and in solving electromagnetic field problems for several waveguide discontinuities. Since 1980 he has been with the Microwave Department of the University of Bremen.

Radial-Symmetric *N*-Way TEM-Line IMPATT Diode Power Combining Arrays

DEAN F. PETERSON, MEMBER, IEEE

Abstract—**Circuit design and stability criteria are developed for a new class of IMPATT diode power combiners. These combiners make use of radial-symmetric circuits and provide an optimal integration of device and circuit properties to perform the power adding function. Both lossless *N*-way combiners and resistively stabilized *N*-way combiners are considered. Theoretical examples of this combining technique are given at *X*-band frequencies which make use of realistic experimentally determined IMPATT diode properties. Predictions for a 30-W ten-diode lossless *X*-band combiner indicate a 1-dB locking bandwidth of 300 MHz and 10-dB gain. A 100-W resistively stabilized 10-GHz ten-diode combiner predicts a 150-MHz locking bandwidth, also at 10-dB locking gain.**

I. Introduction

The purpose of this paper is to present a new approach to circuit-level power combining of negative-resistance devices in general and IMPATT diodes in particular. In a recent review article, the present state of microwave power combining techniques was effectively summarized by Russell [1], to which the reader is referred for an in-depth discussion of various combiner types and their performance. Basically, at the circuit level, combiners can be classified roughly into two categories: *N-way*, in which the outputs from all devices are combined in a single step, and *corporate* (hybrid) or *serial*, in which increasing power levels are successively combined. *N*-way combiners are often additionally separated into resonant and nonresonant structures. Examples of the former are the waveguide combiner of Kurokawa and Megalhaes [2] and the circular cylindrical TM_{0n0} cavities of Harp *et al.* [3]–[6]. Examples of the nonresonant *N*-way combiner include the nonplanar Wilkinson hybrid [7] and the five-way combiner of Rucker [8].

Each of these power combining circuits has its associated performance limitations, design criteria, and problems. Corporate or serial combiners have the advantage of isolation between devices to eliminate deleterious interactions and provide broadband performance, but have the disadvantage of often substantial circuit and combining losses [1], often at high power levels. Resonant *N*-way combiners require stabilization resistors to suppress interactions among devices and undesired oscillation modes in a high-*Q* cavity, leading to narrow-band although high-efficiency combining. Nonresonant *N*-way structures usually provide larger bandwidths with a corresponding increase in the mode suppression problem. Rucker's technique [8] analyzed by Kurokawa [9] has been successful, as has apparently been a conical line technique [10]. Radial arrays of equally spaced TEM lines have been used successfully for transistor power combining [11].

The combining circuits treated in this paper could perhaps be classified as *N*-way nonresonant transmission-line networks. As opposed to other networks of this type, however, the "circuit" and "device" properties are closely intertwined such that each cannot be specified independently. Hence the combiner represents, in some sense, an optimal integration of device and circuit to perform the power adding function. Both lossless and resistively stabilized symmetrical combining circuits are considered and each can provide the desired suppression of the unwanted non-power-producing modes while affording design flexi-

Manuscript received July 2, 1981; revised August 31, 1981. This work was supported by the Air Force Avionics Laboratory, Wright-Patterson Air Force Base, under Contract F33615-77-C-1132.

The author is with the Electron Physics Laboratory, Department of Electrical and Computer Engineering, University of Michigan, Ann Arbor, MI 48109.

0018-9480/82/0200-0163$00.75 ©1982 IEEE

bility in the power-producing mode. Lossless combiners require and make use of the band-limited negative-resistance properties of IMPATT diodes to provide stable and reasonably broad-band operation. Values of TEM-line impedances, lengths, and stabilization resistances are determined by the IMPATT properties, rather than by conventional match and isolation requirements in power adders/dividers [7], [12]. With negative-resistance diode terminations, the concept of "match" in particular is not, *a priori*, a useful condition.

Of particular importance in N-way combiners with active terminations is the suppression of all undesired modes of oscillation. For circuits with certain symmetry properties and identical active terminations, the various modes and their associated oscillation conditions can be specified in all but unusual circumstances [9]. Circuit conditions for avoiding unwanted modes can then be investigated systematically. In Section II, the basic combiner circuit and its symmetry properties are defined. The condition(s) for oscillation are reviewed and specified in terms of circuit eigenvectors and eigenvalues for the case of identical active devices.

Radially symmetric lossless TEM-line combiners having $N-1$ eigenvalue degeneracy are analyzed with examples in Section III. It is shown that diode properties specify combiner TEM-line characteristic impedance and line length for unwanted mode suppression and that circuit design for the power-producing mode is relatively straightforward. An example of a 30-W ten-diode X-band microstrip combiner is given.

Resistive-stabilized TEM-line symmetric combiners are discussed in Section IV. Examples of practical and realizable stabilization networks and their relation to diode and combiner properties are given. Values of stabilizing resistors are specified in terms of device negative conductance level and the number of diodes combined. As an example, a detailed analysis of a 100-W ten-diode X-band microstrip combiner is presented.

II. Combiner Description and Stability Considerations

A. Combiner Description

A general power combining network for use with negative-resistance devices is shown in Fig. 1. The combiner has N ports for active device terminations and one port for common excitation and output power extraction. It is assumed that the combiner has certain symmetry properties such that its admittance matrix $\boldsymbol{Y}_c$ can be written as

$$\boldsymbol{Y}_c = \begin{bmatrix} y_{00} & y_{0d} & y_{0d} & \cdots & y_{0d} \\ y_{0d} & & & & \\ y_{0d} & & & & \\ y_{0d} & & & \boldsymbol{Y} & \\ \vdots & & & & \\ y_{0d} & & & & \end{bmatrix} \tag{1}$$

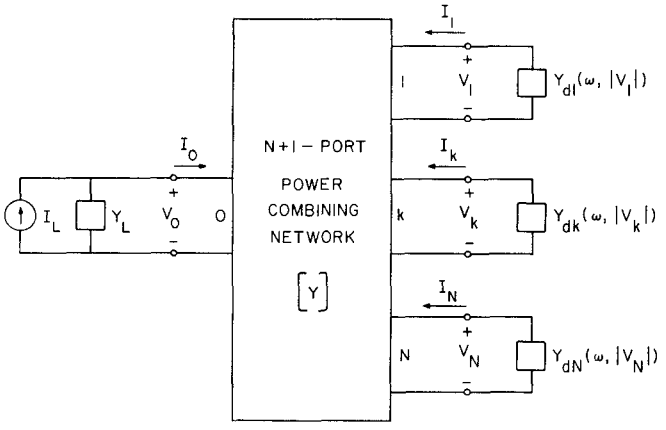

Fig. 1. A general N-negative-resistance-diode power-combining network.

where the $N \times N$ matrix $\boldsymbol{Y}$ defined as

$$\boldsymbol{Y} \triangleq [y_{mn}] \tag{2}$$

has the element properties that

$$y_{m+k,n+k} = y_{mn} = y_{nm} \tag{3}$$

where the subscripts are modulo N.[1] Such a matrix is called a "circulant" [13] indicating the combiner has radial symmetry with any row of $\boldsymbol{Y}$ a "rolled" version of any other row. Along with reciprocity, this implies that $\boldsymbol{Y}$ has at most $N/2+1$ distinct elements if N is even and $(N+1)/2$ distinct elements if N is odd. Except for certain hybrids, resonant cavity [2] and graduated coupling structures, most useful power combiners have the symmetry properties indicated above.

B. Terminations

Ports 1 through N of the combiner will be terminated in active, nonlinear devices. It is assumed that the device on port $k, 1 \leq k \leq N$ can be represented by its admittance describing function $Y_{dk}(\omega, |V_k|)$, where $|V_k|$ is the *amplitude* of the RF voltage at port k and ω is the frequency. At port 0, the termination is $Y_L(\omega)$ with current excitation I_L. The termination matrix $\boldsymbol{Y}_t$ is thus written as

$$\boldsymbol{Y}_t = \operatorname{diag}\left[Y_L(\omega), Y_{d1}(\omega, |V_1|), \cdots, Y_{dN}(\omega, |V_N|)\right]. \tag{4}$$

C. Condition for Oscillation

Of particular interest for multidiode combiners is system stability when devices are capable of interacting with one another. The condition for oscillation for the combiner can be written as

$$(\boldsymbol{Y}_c + \boldsymbol{Y}_t)\boldsymbol{V} = \boldsymbol{0} \tag{5}$$

where

$$\boldsymbol{V} = [V_0 V_1 V_2 \cdots V_N]^t \tag{6}$$

is the vector of port voltages and $\boldsymbol{0}$ is the empty vector. For

[1] Take on values from 1 to N only.

a given termination Y_L at port 0

$$V_0 = -\frac{y_{0d}\sum_{k=1}^{N} V_k}{y_{00}+Y_L} \tag{7}$$

and the condition for oscillation becomes

$$(\boldsymbol{Y}'+\boldsymbol{Y}_t')\boldsymbol{V}'=\boldsymbol{0}' \tag{8}$$

where the primed quantities are associated only with ports 1 to N, and the elements of $Y'=[y'_{mn}]$ are given by

$$Y'_{mn} = y_{mn} - \frac{y_{0d}^2}{y_{00}+Y_L}. \tag{9}$$

The matrix $\boldsymbol{Y}'$ retains the symmetry properties of $\boldsymbol{Y}$. Nontrivial solutions to (8) are the modes of oscillation for the system.

D. Modes of Oscillation

The eigenvectors $\boldsymbol{x}_k$ and associated eigenvalues λ_K for the symmetric circulant matrix $\boldsymbol{Y}'$ are obtained from

$$\boldsymbol{Y}'\boldsymbol{x}_k = \lambda_k \boldsymbol{x}_k \tag{10}$$

and are given by

$$\boldsymbol{x}_k = \frac{1}{\sqrt{N}}\begin{bmatrix} 1 \\ e^{jka} \\ e^{j2ka} \\ \vdots \\ e^{j(N-1)ka} \end{bmatrix}, \qquad k=0 \text{ to } N-1 \tag{11}$$

and

$$\lambda_k = \sum_{n=1}^{N} y'_{mn} e^{jka(n-1)}, \qquad k=0 \text{ to } N-1, \qquad \text{any } m \tag{12}$$

where $a=2\pi/N$. The eigenvector $\boldsymbol{x}_0$ and corresponding eigenvalue λ_0 are associated with the in-phase desired power-producing mode for the combiner, while the other $\boldsymbol{x}_k$ and λ_k are associated with "rotating" or anti-phase modes of no output. Using (9) in (12) shows that

$$\lambda_0 = \sum_{n=1}^{N} y_{mn} - \frac{N y_{0d}^2}{y_{00}+Y_L}, \qquad \text{any } m \tag{13a}$$

and

$$\lambda_k = \sum_{n=1}^{N} y_{mn} e^{jka(n-1)}, \qquad \text{any } m, \qquad k=1 \text{ to } N-1. \tag{13b}$$

Hence, the $\lambda_k, 1 \leq k \leq N-1$ are the same for the matrices $\boldsymbol{Y}$ and $\boldsymbol{Y}'$ and are independent of the load admittance. The number of distinct eigenvalues is the same as the number of distinct values of the y_{mn}, which is $N/2+1$ for N even and $(N+1)/2$ if N is odd.

Possible solutions to (8) are now seen to be

$$-\boldsymbol{Y}_t' = \lambda_k \boldsymbol{I} \quad \text{for} \quad \boldsymbol{V}' = \sqrt{N}\, V \boldsymbol{x}_k \tag{14}$$

where $\boldsymbol{I}$ is the identity matrix and $V=|V_n|, 1 \leq n \leq N$. Equivalently,

$$-Y_{dn}(j\omega, |V_n|) = -Y_d(j\omega, V) = \lambda_k(j\omega) \tag{15}$$

i.e., all Y_{dn} are the same. In this case, the zeroth mode (λ_0) is the power-producing mode and would require a stable solution to

$$-Y_d(j\omega, V) = \lambda_0(j\omega) \tag{16}$$

for oscillation. Any stable antiphase modes characterized by $\Sigma V_k = 0$ [$V_0 = 0$ from (7)] would need to be suppressed for the combiner to operate properly. In this case of identical active devices, circuit design must provide the proper value of λ_0 for oscillation or amplification while suppressing the other modes. Since the λ_k in (13b) are independent of Y_L and depend only on the inherent properties of the combiner circuit, a stable, even-mode-only design is possible in principle.

E. Other Modes

Additional modes to those outlined above are possible in the combiner because the devices are nonlinear and can be nonidentical. One such mode, pointed out by Kurokawa [9], was based on a perturbation analysis and found to be very unlikely to exist because of the device-circuit relation required. The case of other modes is treated extensively in [14], where more general stability conditions than Kurokawa's are derived. The results seem to indicate that other modes would require unusual conditions between the device and circuit properties, at least when the devices are nearly identical.

III. Lossless Radial-Symmetric TEM-Line IMPATT Combiners

A. Degenerate Eigenvalue Networks

A combining network which is lossless and obeys the symmetry properties given in Section II has eigenvalues $\lambda_k, 1 \leq k \leq N$, that are purely imaginary since the y_{mn} in (13b) are all imaginary. Clearly, for the rotating modes, all the power into the network must be returned. Hence, rotating mode suppression in an active diode combiner requires the device to be stable under the lossless terminations representative of the combiner network λ_k's.

This criterion can be achieved using the IMPATT diodes and a simple TEM-line power-combining circuit. Under certain conditions, the *band-limited negative-resistance* properties of IMPATT diodes in combination with TEM lines of suitable length and characteristic impedance can provide a stable combiner in which only the even mode can exist.

The simplest combiner of this type is a TEM-line network as shown in Fig. 2. An array of identical transmission lines is placed symmetrically around a "hub" where power is extracted, with the lines terminated in IMPATT diodes. For this network, it is assumed that

$$y_{mn} = 0, \qquad m \neq n \tag{17}$$

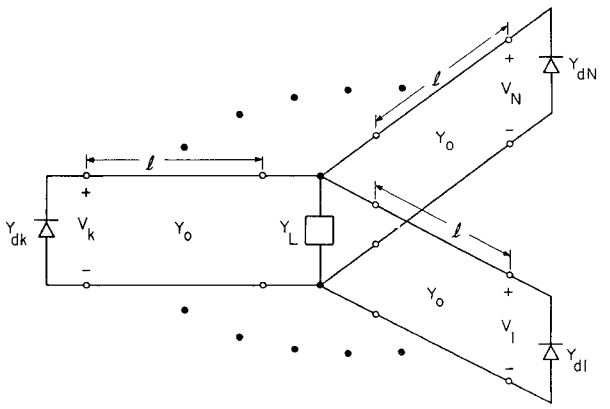

Fig. 2. A TEM-line combining network providing $N-1$ degenerate eigenvalues for the rotating modes.

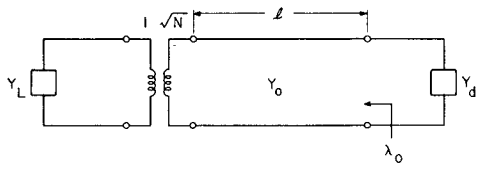

Fig. 3. An equivalent circuit for the N-diode TEM-line combiner from an admittance point. The power in Y_L is N times the power generated by Y_d.

so that the eigenvalues λ_k are degenerate and

$$\lambda_k = y_{11}(j\omega) = -jY_0 \cot \beta l, \qquad 1 \leqslant k \leqslant N \tag{18}$$

for all the rotating modes. The eigenvalue λ_0 associated with the even mode is then given by

$$\lambda_0 = -jY_0 \cot \beta l + \frac{NY_0^2 \csc^2 \beta l}{Y_L - jY_0 N \cot \beta l} \tag{19}$$

where β is the propagation factor, so that λ_0 represents the input admittance of a TEM line terminated in an effective admittance of Y_L/N (see Fig. 3).

The assumption of eigenvalue degeneracy and zero coupling between lines simplifies the design problem and illustrates the appropriate device-circuit interaction for stability. This criteria can be approximately met in practice, especially if the number of diodes is not too large. For slight coupling between lines, such that the eigenvalues are not too different, an appropriate design can still be achieved in many cases. This point will be clarified later in this section.

B. Rotating Mode Stability

Stability of the rotating modes for the degenerate case requires that there be no *stable* solutions to

$$Y_d(j\omega, V) - jY_0 \cot \beta l = 0 \tag{20}$$

for any combination of ω and V, where identical diodes have been assumed. Equivalently,

$$\mathrm{Re}\{Y_d(j\omega, V)\} \triangleq G_d(\omega, V) = 0 \tag{21a}$$

$$\mathrm{Im}\{Y_d(j\omega, V)\} \triangleq B_d(\omega, V) = Y_0 \cot \beta l. \tag{21b}$$

If $V_0(\omega)$ is the voltage required at any ω to satisfy (21a),

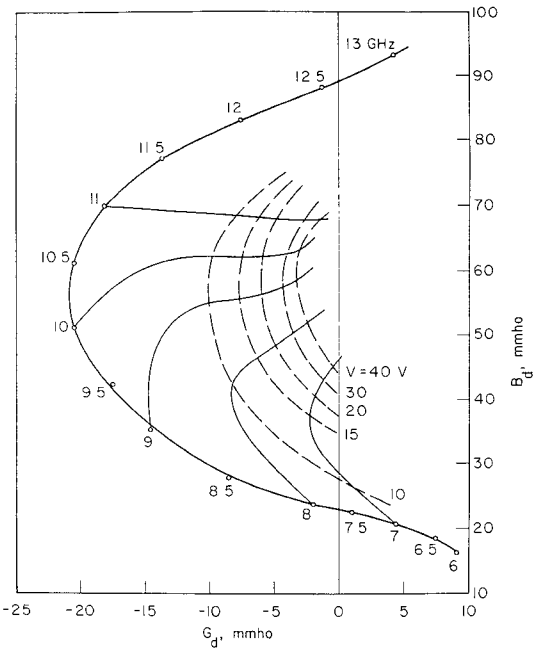

Fig. 4. Typical admittance plane plot of the nonlinear properties of an IMPATT diode, in this case a 2.5-W X-band Read device as determined experimentally.

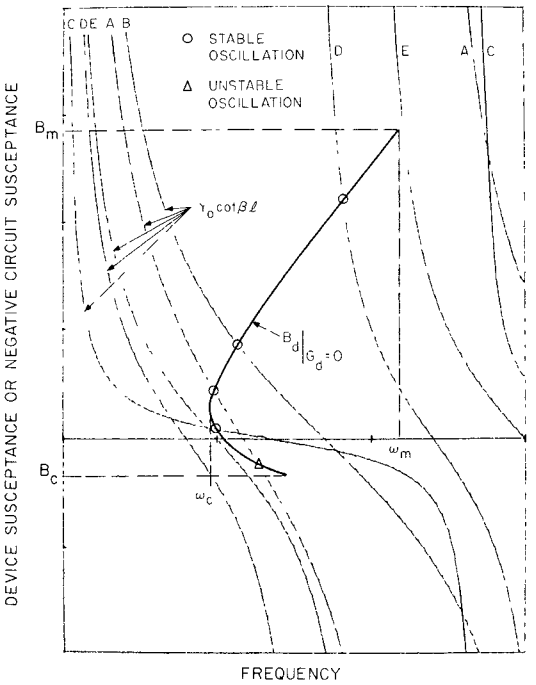

Fig. 5. Device-circuit interaction pertinent to rotating mode stability showing a typical $B_{dg}(\omega)$ plot [B_d for $G_d(V)=0$] and several circuit negative susceptances for a TEM-line combiner. Only circuit curve E is a stable situation.

then the associated diode susceptance $B_{dg}(\omega)$ is obtained as

$$B_{dg}(\omega) = B_d[\omega, V_0(\omega)]. \tag{22}$$

Since the IMPATT diode has a band-limited negative conductance, any solutions to (20) or (21) need be considered only over a certain band of frequencies. A typical plot of the nonlinear admittance properties of an IMPATT diode is shown in Fig. 4, indicating the limited negative-

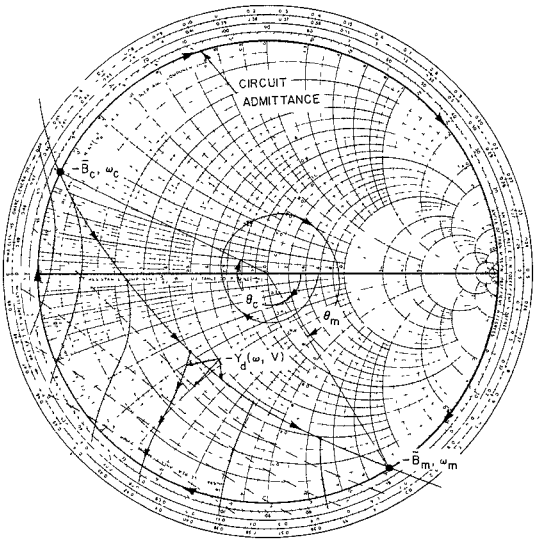

Fig. 6. Stability conditions interpreted on the Smith chart showing the defined angles θ_c and θ_m and the circuit admittance.

resistance bandwidth. The conductance first becomes negative near the "avalanche" frequency, goes through a maximum and becomes positive again at a frequency determined by the device carrier transit time. Of importance in (20) or (21) is that large-signal levels *can decrease* the diode conductance, *especially* at the lower frequencies. In fact, a passive admittance at small-signal levels can become active for certain drive levels and frequencies. As evident, the effect of this is to make the solution to (21a) double valued, providing two values of B_{dg} at some frequencies. This must be considered when designing to avoid the conditions of (20) or (21).

Several types of device and circuit interactions are indicated in Fig. 5, where $B_{dg}(\omega)$ is compared to several circuit functions $Y_0 \cot \beta l$. Dispersionless TEM lines are assumed. The maximum frequency of zero conductance is ω_m and the minimum frequency is ω_c. The end points of the B_{dg} curve correspond to solutions of (21a) with $V=0$ (small signal). Circuit functions A through D all result in solutions to (20) from improper selection of Y_0 and/or line length l. Only circuit admittance E will provide a stable situation. From Fig. 4 it is quite clear that stability can be avoided by choosing Y_0 and l such that

$$Y_0 \cot \beta(\omega_c) l \leq B_c \tag{23a}$$

and

$$Y_0 \cot \beta(\omega_m) l \geq B_m \tag{23b}$$

where B_c and B_m are defined in Fig. 5. Using B_c and ω_c as shown in Fig. 5 is sufficient in (23a) but not always necessary as apparent from curve E. The best choice for B_c and ω_c depends on the nature of B_{dm} for the devices considered.

Conditions (23) can perhaps be visualized somewhat easier on the Smith chart as shown in Fig. 6, where $-B_{dg}/Y_0 = -\bar{B}_{dg}$ is compared to $-\cot \beta l$. The circuit appears as a length of shorted TEM line and the angle $\theta(\omega)$ of its normalized admittance measured as shown is simply $2\beta(\omega)l$. Hence, stability requires that $\theta(\omega_c) \geq \arg(-\bar{B}_c)$ and $\theta(\omega_m) - 2\pi < \arg(-\bar{B}_m)$. This translates unambiguously to the stability conditions given by

$$\theta(\omega_c) \triangleq \theta_c \geq \pi + 2\tan^{-1}(-\bar{B}_c) \tag{24a}$$

$$\theta(\omega_m) \triangleq \theta_m \leq 2\pi - 2\tan^{-1}(-1/\bar{B}_m) \tag{24b}$$

where the $\tan^{-1}$ is either in the first or fourth quadrant. The line length l determines the values of θ_c and θ_m and the normalization admittance scales the values of $\bar{B}_c$ and $\bar{B}_m$. An appropriate combination can often provide stability. Since β varies essentially linearly with frequency, it is apparent from Figs. 5 or 6 that the diode must have $\omega_m/\omega_c \approx 2$ in order to satisfy (24). Other solutions to (23) are possible, but these require either unrealistically short line lengths or long line lengths and narrow active device bandwidths. The situation indicated by Fig. 5 or Fig. 6 is the only practical solution. Additional stability margin and design flexibility can be afforded by the use of parallel capacitance across the diode and two-section TEM-line networks [14].

C. Even-Mode Design Considerations

Within the confines imposed by the stability constraints above, certain considerations should be given to the even-mode oscillator or amplifier design. For the circuit of Fig. 2, each diode admittance will be rotated through the length of TEM line and added to $N-1$ essentially identical admittances at the combining point. An equivalent circuit for this is shown in Fig. 3, assuming identical diodes. Practical considerations dictate that the total admittance level at the combining point should have reasonable values around the design frequency. Since adding together N diodes acts like an ideal impedance transformer, the optimum situation is to have the admittance real at the design frequency in an antiresonance mode. Again, the nature of the IMPATT admittance and the TEM-line lengths required for mode stability can often allow this condition to be met, making realization of the desired load admittance Y_L straightforward.

D. Diode Design Considerations

The combining technique indicated here requires proper design of both diode and circuit. Circuit design flexibility is enhanced by using diodes which have active bandwidths $\omega_m/\omega_c \cong 2$ and optimum frequencies appropriate for simplified even-mode design. Fortunately, the design of IMPATT diodes and the technology for fabricating them has advanced to the point where the above device goals are likely achievable. With the proper doping profile and bias current density ω_c, ω_m and the design frequency can be controlled to simplify combiner design. An example of a combiner design using this method is now given.

E. A Theoretical Ten-Diode X-Band 25-W Microstrip Combiner

The admittance properties $Y_d(j\omega, V)$ of an X-band GaAs Read HI-LO IMPATT diode used for a design example are

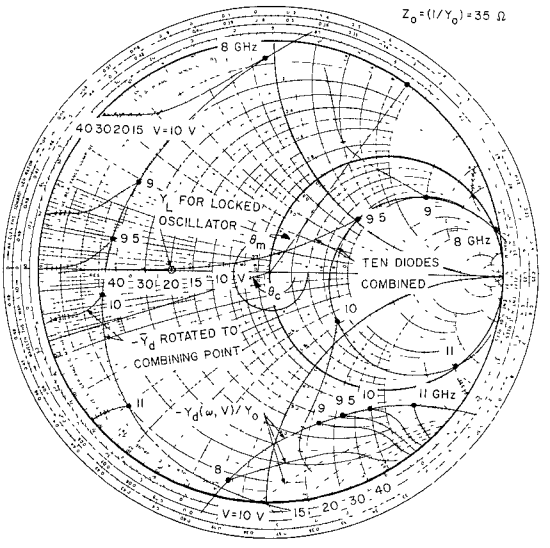

Fig. 7. Normalized diode characteristics of Fig. 4 before and after line rotation to the combining point. Also shown is the result of combining ten diodes. The value of $\bar{Y}_L$ chosen was for a locked oscillator gain of approximately 10 dB at 9.5 GHz for ten diodes.

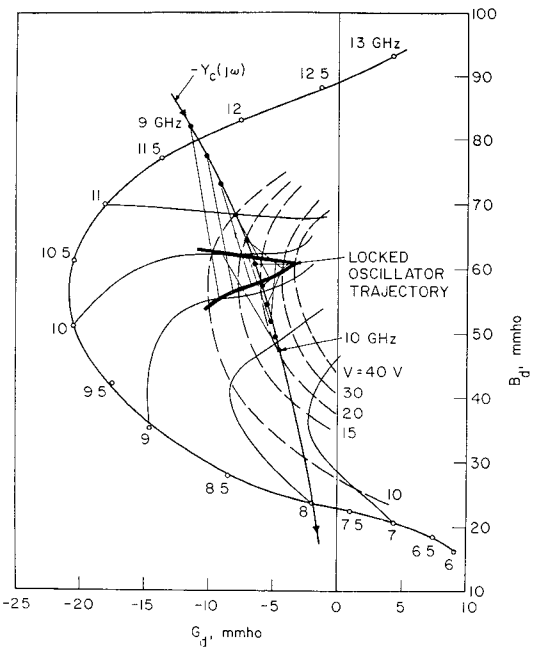

Fig. 8. Device–circuit interaction shown in device admittance plane for the X-band locked oscillator. The locked oscillator trajectory is also shown.

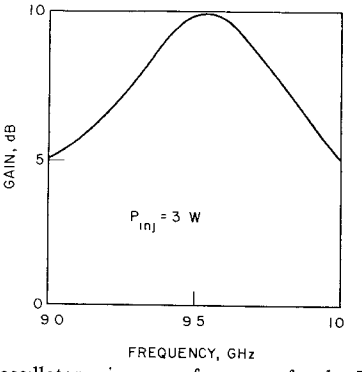

Fig. 9. Locked oscillator gain versus frequency for the X-band oscillator at a constant RF locking signal power of 3 W. The 1-dB bandwidth is almost 300 MHz.

shown in Fig. 4. These characteristics were determined experimentally using large- and small-signal measurements and de-embedding techniques. For this diode, the dc bias current was 150 mA with a voltage of approximately 66 V under large-signal conditions. The optimum frequency and RF voltage level are at 9.5 GHz and 40 V, respectively, providing an output power of 2.64 W at approximately 27-percent efficiency.

As seen from Fig. 4, both B_m and B_c are positive and the active bandwidth $\omega_m/\omega_c<2$, allowing substantial freedom in the choices of Y_0 and l for the combining lines. Appropriate choices for these parameters can thus be made so that the optimum power admittance for the diode viewed at the common combining point will lie on the real axis with a normalized admittance value less than unity. For this design, a choice of $Z_0=1/Y_0$ of 35 Ω was used with $\theta_c=2.83$ and $\omega_c=6.7$ GHz. This choice results in the optimum power point at 9.5 GHz to lie on the real axis at the combining point.

Shown on the Smith chart of Fig. 7 are the normalized diode admittance characteristics before and after rotation through the line to the combining point and the characteristics resulting from a ten-diode combiner. It should be clear why the optimum power point should lie on the real axis for simplest oscillator/amplifier design. Optimum oscillator performance at 9.5 GHz for the ten-diode combiner now requires a load admittance of $Y_L=0.2$, $Y_0=0.0057$, or $Z_L=175$ Ω. This could easily be realized by using a $\lambda/4$ transformer from a 50-Ω output impedance level.

As a stable amplifier, this combiner would have very low gain since the normalized load admittance would have to be greater than 1.8 to avoid any oscillation, as can be seen from Fig. 7. However, the combiner could be used as an injection-locked oscillator to provide maximum diode power capability with any desired locking gain. As an example of expected performance as a locked oscillator, a normalized load admittance of 0.4 was selected to achieve approximately 10 dB of locking gain at 9.5 GHz with an optimum input RF level of 3 W. The locking trajectory on the device curves as a function of frequency is shown in Fig. 8 from 9 to 10 GHz. This trajectory was obtained by graphically solving the locking equation

$$Y_d(j\omega_l, V)+Y_c(j\omega_l)=\frac{I_L}{V} \tag{25}$$

where Y_c is the circuit admittance seen by the diode and I_L is the equivalent locking source related to the injected power P_L by

$$|I_L(\omega_l)|=\sqrt{8G_c(\omega_l)P_L}\,. \tag{26}$$

From the analysis, the predicted power versus frequency response of the locked oscillator is indicated in Fig. 9 for a constant RF power input of 3 W. The peak output power is

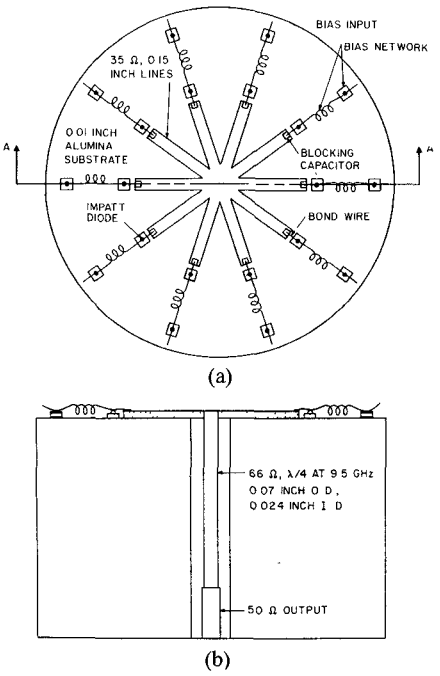

Fig. 10. A possible microstrip realization of the TEM-line combiner of Figs. 8 and 9.

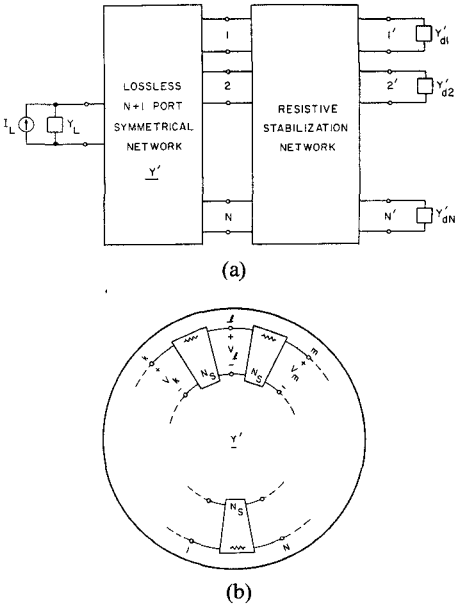

Fig. 11. (a) A general resistive stabilization network added to a symmetrical lossless $N+1$ port combiner. The primed admittances indicate possible lossless circuit transformations. (b) The form of the stabilization networks in (a) which will be considered. Radial symmetry is assumed.

30 W at 9.5 GHz with a 3-dB bandwidth of approximately 600 MHz.

A proposed microstrip realization of the ten-diode combiner is shown in Fig. 10. In the analysis above, the effect of bond wires and the bias network needed were neglected. However, there is so much design margin with the diodes used that proper design of these elements will not affect rotating mode stability. Line lengths can be shortened appropriately to account for bonding lead inductance. Coupling among the various combiner lines will provide nondegenerate eigenvalues which will be shifted somewhat from the degenerate value. For the expected small coupling, this shift can be handled by the design margin.

IV. Resistive-Stabilized Radial-Symmetric Combiners

A. Circuit Description

Resistive stabilization networks embedded into the $N+1$ port diode power combiner can provide increased design flexibility over the lossless case while still retaining rotating mode suppression properties. The penalty is typically an increase in combiner size and stored energy to accommodate the stabilization with a corresponding reduction in combiner bandwidth. In addition, the circuitry becomes more complex, although the use of chip resistors and planar microstrip geometry results in fairly straightforward circuit designs.

Maximum advantage of resistive stabilization is possible if the circuit retains its symmetry properties as outlined in Section II. The type of stabilization schemes utilized here are indicated in Fig. 11(a) and (b). Basically, a lossless $N+1$ port combiner is augmented by a symmetrical resistive stablization network as in Fig. 11(a). The use of primed diode admittances indicates that the diodes may be themselves embedded in a lossless network before stabilization occurs. In Fig. 11(b), the form of the stabilization network is given showing the use of identical two-port symmetrical lossy networks N_s sequentially connected from port to port of the lossless combining network of Fig. 11(a). Such stabilization could easily be implemented in radial-symmetric planar networks. The properties of these networks can be specified so that all rotating modes are suppressed by resistive loading, while even-mode combining remains lossless.

B. Stabilization Networks and Combiner Eigenvalues

The form of the stabilization does not change the symmetry properties of the combining network and the eigenvectors of the new network will remain unchanged. The eigenvalues will, however, be modified by the presence of N_s and the new eigenvalues $\lambda'_n, 0 \leq n \leq N-1$ can easily be found by making use of the eigenvectors.

With reference to Fig. 11(b), the equivalent circuit model used at the sequential combiner ports k, l, and m for eigenvector or mode n is shown in Fig. 12(a). It is required that the port-to-port networks be symmetrical and λ_n is the nth eigenvalue of the lossless, unstabilized combiner network. Furthermore, the stabilization network is assumed to be of the form indicated in Fig. 12(b), where G_s represents a stabilization conductance (chip resistor) placed between mirror image lossless networks. These networks from combiner port to the stabilization resistor are characterized by a Y-matrix $\boldsymbol{Y}_b$ of the form

$$\boldsymbol{Y}_b = \begin{bmatrix} y_{aa} & y_{ab} \\ y_{ab} & y_{bb} \end{bmatrix} \tag{27}$$

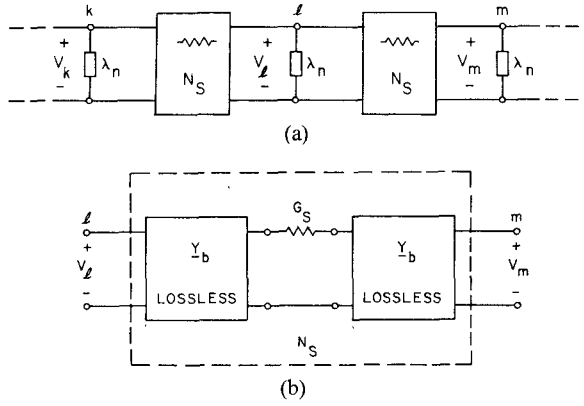

Fig. 12. (a) The equivalent circuit model at the ports k, l, and m for eigenvector or mode n of the symmetrical combiners. λ_n is the corresponding eigenvalue for the lossless combiner portion. (b) The form assumed for port-to-port stabilization networks N_s of (a). The networks Y_b are lossless and mirror images.

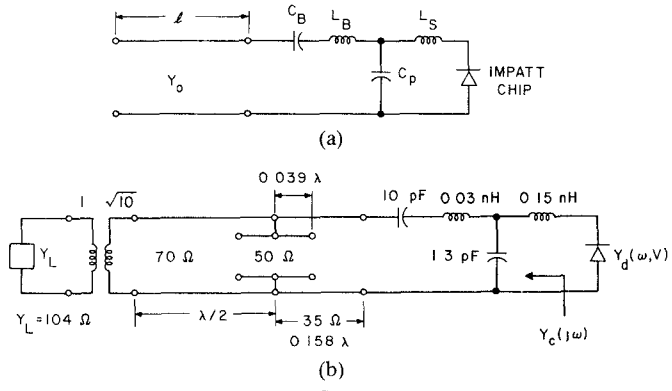

Fig. 13. (a) Impedance transformation used to obtain Y_d' at the terminals of the stabilization networks. The diode admittance properties are shown in Fig. 4 except the scales are increased by a factor of four. (b) Equivalent circuit for the resistive stabilized ten-diode combiner in the even mode where the stabilization resistances are invisible. For this combiner, $G_s = 0.01\,\mathcal{O}$.

in which y_{aa} and y_{bb} are not necessarily equal.

The new eigenvalues can now be found from the requirement that

$$V_k = e^{-jna} V_l \tag{28a}$$

and

$$V_l = e^{-jna} V_m. \tag{28b}$$

Analysis of the circuit of Fig. 12(a) with decomposition as in Fig. 12(b) with the voltage constraints above shows that λ_n' is given by

$$\lambda_n' = \lambda_n + Y_{ns} \tag{29}$$

where

$$Y_{ns} = 2\left[y_{aa} - \frac{y_{ab}^2}{y_{bb}} + \frac{y_{ab}^2}{y_{bb}} \frac{G_s(1-\cos na)}{y_{bb}+2G_s} \right]. \tag{30}$$

As expected, for the zeroth (even) mode, Y_{0s} is just twice the open circuit admittance of the lossless network Y_b which is purely imaginary. Of course λ_0 is a positive real admittance since this is the combining mode. For all the rotating modes, $\mathrm{Re}\{\lambda_n\} = 0$ but $\mathrm{Re}\{Y_{ns}\} > 0$ because of G_s, and stabilization of these modes is possible with the proper selection of G_s and Y_b so that

$$Y_d'(j\omega, V) + \lambda_n'(j\omega) = 0 \tag{31}$$

is not satisfied for any ω, V where the diode is active.

C. TEM-Line Stabilization Networks

A case of practical interest is to have Y_b be represented by a TEM line of length l_s and characteristic admittance Y_s so that

$$y_{aa} = y_{bb} = -jY_s \cot \beta l_s \tag{32a}$$

and

$$y_{ab} = \pm jY_s \csc \beta l_s. \tag{32b}$$

Use of (32) in (30) shows that

$$G_{ns} = \mathrm{Re}\{Y_{ns}\} = 2G_s(1-\cos na) \frac{1+\tan^2 \beta l_s}{1+\left(\frac{2G_s}{Y_s}\right)^2 \tan^2 \beta l_s}. \tag{33}$$

As a function of frequency, G_{ns} oscillates between minimum and maximum values occurring when βl_s takes on integral values of $\pi/2$. Simplified design for mode stability is possible if G_{ns} is made independent of frequency by choosing

$$\frac{2G_s}{Y_s} = 1 \tag{34}$$

so that

$$G_{ns} = 2G_s(1-\cos na). \tag{35}$$

Stability of mode n is then accomplished simply by having

$$G_{ns} > -G_{d,\min}' \tag{36}$$

where $G_{d,\min}' = \min\{\mathrm{Re}[Y_d'(j\omega, V)]\}$ or the diode minimum negative conductance. Using (36) in (35) requires

$$G_s > -\frac{G_{d,\min}'}{2(1-\cos na)} \tag{37}$$

which must hold for all rotating modes. The worst case occurs when $na = \pm 2\pi/N$ ($n = 1$ or $N-1$) requiring

$$G_s = \frac{Y_s}{2} > -\frac{G_{d,\min}'}{2\left(1-\cos\frac{2\pi}{N}\right)} \tag{38}$$

for overall stability.

In order to make use of realizable line admittance values Y_s, the diode admittance Y_d may have to be transformed through a low-loss network to Y_d' such that (37) can be satisfied in a practical fashion. In such a transformation, the number of diodes N is also a factor.

For the desired even mode, the stabilization network results in two parallel open circuit stubs across the (transformed) diode of length l_s and characteristic admittance Y_s. The length of these lines can be used effectively in combination with the rest of the circuit for tuning and impedance

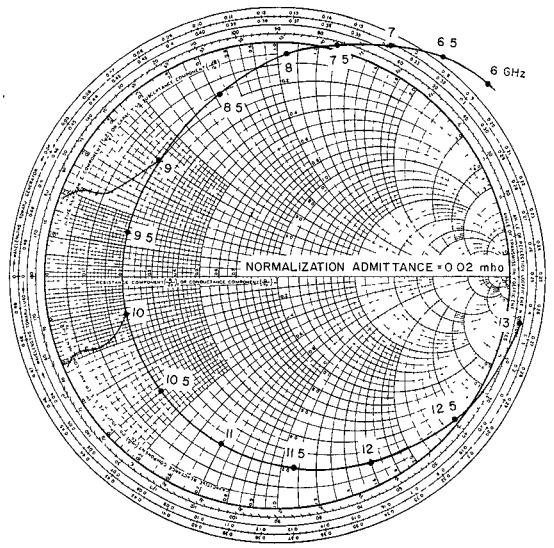

Fig. 14. The diode admittance properties rotated to the combining point where the circuit is as shown in Fig. 13(b). The admittance is resonant at approximately 9.5 GHz.

matching purposes in the even-mode combiner circuit design.

D. A Theoretical Ten-Diode 100-W X-Band Combiner

For this example, the IMPATT devices with characteristics shown in Fig. 4 were again used except each diode was assumed to be four times as large. Therefore, the admittance of the device would be scaled (increased) by four as would the RF power capability, providing 10 W per diode. The size increase could be obtained by doubling the diode diameter if the associated thermal resistance was consistent, or more likely by using a diode "quad." With such a large device and the resulting low impedance level, the lossless TEM combiner becomes impractical or unrealizable. It is impractical because with chip devices the line impedances required would be too low to realize effectively, and if a low-loss impedance transformer is used on the chip, the resulting increased reactance variation makes rotating mode stability difficult or impossible. Hence, a stabilized design is required for a reasonable and realizable solution for the combiner.

The low impedance level of the diode dictates a low-loss *LC* impedance level transformation near the diode for matching purposes, at some expense in bandwidth. In addition, at the stabilization point, the peak negative conductance of the transformed diode must relate to the stabilization line admittance Y_s as in (38), i.e.,

$$-G_{d,\min} < Y_s\left(1-\cos\frac{2\pi}{N}\right) = Y_s, \qquad N=10 \qquad (39)$$

where Y_s represents a practical admittance level ($\sim 0.02\,\Omega$). To satisfy (39) with $Y_s \approx 0.02\,\Omega$, the circuit of Fig. 13(a) was assumed and the package parasitics and line parameters were adjusted such that $-G_{d,\min}$ occurred at the design frequency of 9.5 GHz. Bonding inductance and blocking capacitance are modeled by L_B and C_B, although their effect is minimal. The parameter values used are indicated in Fig. 13(b).

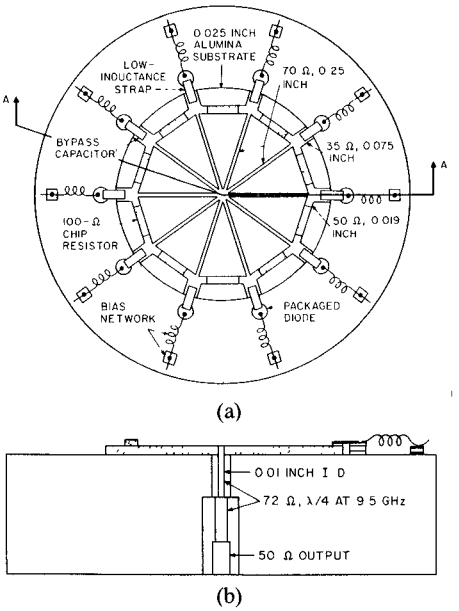

Fig. 15. A possible microstrip circuit realization of the combiner of Fig. 13(b) including the use of packaged devices with proper parasitics and biasing networks.

The stabilizing line lengths were selected to provide a parallel resonance at 9.5 GHz, and the resulting admittance was mapped through a half-wavelength line at 9.5 GHz to the combining point. Hence, the total admittance at the combining point adds to a reasonable and realizable value. The negative admittance of the active device at the stabilization point, including the effect of the stubs, is shown on the Smith chart plot of Fig. 14. The equivalent circuit for the combiner is shown in Fig. 13(b), and a possible microstrip realization is given in Fig. 15. Bias circuit elements indicated in Fig. 15 were assumed negligible in the analysis. It may be necessary to use the "bias circuit" elements for subharmonic suppression by providing a series resonance at the half frequency in addition to a high imped-

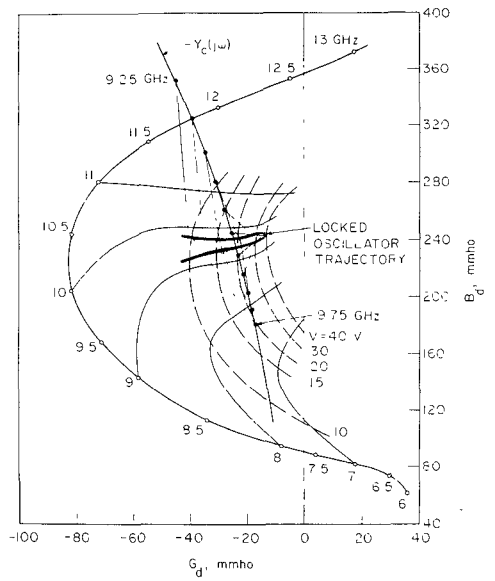

Fig. 16. Device–circuit interaction for the circuit of Fig. 13(b) with Y_L adjusted for 10 dB of locked oscillator gain at 9.5 GHz. This plot can be compared to that of Fig. 9.

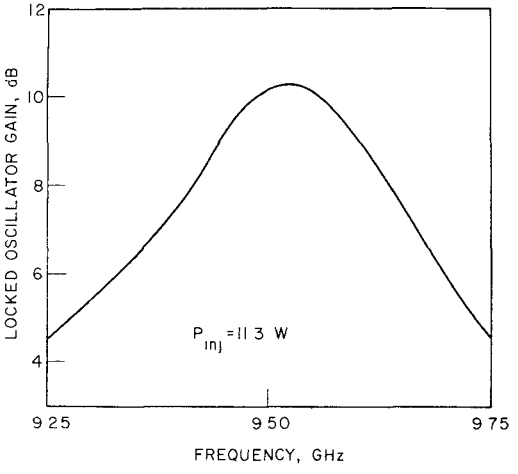

Fig. 17. Locked oscillator gain versus frequency obtained from the curve of Fig. 16 The 1-dB bandwidth has reduced to 150 MHz for the factor of four increase in power output.

ance at 9.5 GHz. The value of Y_L indicated was chosen for 10 dB of locking gain at 9.5 GHz.

Shown in Fig. 16 are the device admittance curves, the circuit admittance $Y_c(j\omega)$, and the locked oscillator trajectory for a peak locking gain of 10 dB at 9.5 GHz and maximum RF power. The bandwidth reduction from the previous lower power lossless design is apparent.

Total expected combiner output power as a function of frequency is shown in Fig. 17, indicating a peak output level of 117 W at 9.5 GHz and 10-dB gain. As before, the injected power level was held constant across the band, in this case being 11.3 W. The 3-dB bandwidth is approximately 270 MHz.

V. Summary and Conclusions

The combining circuits studied in this report differ from other designs primarily because the circuit design is more heavily constrained by the device properties. In this sense, the "device" and "circuit" are not separate entities, but are "matched" to each other's properties to optimally perform the power adding function. Combiners studied were of two basic types: lossless radially symmetric TEM-line circuits and resistive stabilized symmetric TEM-line combiners. In the former case, combiner even-mode stability required certain device and circuit properties which, when achieved, led to small size, low stored energy, potentially high-power combiners as shown by the 10-GHz example. Such combiners are ideally suited to integrated circuit techniques. Resistive stabilization of the combiner circuit is required for use with packaged devices or in the case of large active device bandwidths in order to achieve stability. For the symmetrical circuit case, a simple technique is available for determining the value and location of stabilization resistors which suppress odd modes but are invisible to even modes.

Again, the design of these combiners is not based on the conventional concepts of "match" and "isolation" useful in other power dividing/adding arrays of sources or amplifiers. The negative-resistance properties of the device bring about new and more appropriate constraints on line impedance levels, lengths and stabilization (isolation) resistances.

It is concluded from this work that this approach to power combining can potentially provide as good and often better performance than other combining schemes [1]. At X-band, the lossless combiner demonstrated a locked oscillator bandwidth several times larger than TM_{0n0}-mode combiners in a simple r geometry. Use of "fork" style combiners rather than radial-symmetric types are likely candidates for combiner integrated circuit realizations of this type at millimeter wavelengths.

Acknowledgment

The author wishes to express his appreciation to Professor G. I. Haddad for his contribution to this work.

References

[1] K. J. Russell, "Microwave power combining techniques," *IEEE Trans. Microwave Theory Tech.*, vol. MTT-27, pp. 472–478, May 1979.

[2] K. Kurokawa and F. M Magalhaes, "An X-band 10-watt multiple-IMPATT oscillator," *Proc IEEE*, vol. 59, pp. 102–103, Jan. 1971.

[3] R S. Harp and H. C. Stover, "Power combining of X-band IMPATT circuit modules," in *IEEE Int. Solid-State Circuits Conf. Dig.*, (Philadelphia, PA), 1973, pp. 118–119.

[4] "Microwave Power Combinatorial Development, Task I: 10 GHz Amplifier/Combiner," Final Tech. Rep. No. AFAL-TR-75-175, Nov. 1975.

[5] R. S Harp and K. J. Russell, "Improvements in bandwidth and frequency capability of microwave power combinatorial techniques," in *IEEE Int Solid-State Circuits Conf. Dig.*, (Philadelphia, PA), Feb. 1974, pp. 94–95.

[6] K. J. Russell and R. S. Harp, "Power combiner operation with pulsed IMPATT's," in *IMPATT Int. Solid-State Circuits Conf. Dig.*,

(Philadelphia, PA), Feb. 1975, pp. 136–137.
[7] E. Wilkinson, "An N-way hybrid power divider," *IRE Trans. Microwave Theory Tech.*, vol. MTT-8, pp. 116–118, Jan. 1960.
[8] C. T. Rucker, "A multiple-diode, high-average power avalanche-diode oscillator," *IEEE Trans. Microwave Theory Tech.*, vol. MTT-17, pp. 1156–1158, Dec. 1969.
[9] K. Kurokawa, "An analysis of Rucker's multidevice symmetrical oscillator," *IEEE Trans. Microwave Theory Tech.*, vol. MTT-18, pp. 967–969, Nov. 1970.
[10] K. J. Russell and R. S. Harp, "Broadband diode power-combining techniques," Air Force Avionics Laboratory, Wright-Patterson Air Force Base, OH, Interim Tech. Rep. No. 1, Mar. 1978.
[11] J. M. Schellenberg and M. Cohn, "A wideband radial power combiner for FET amplifiers," in *IEEE Int. Solid-State Circuits Conf. Dig.*, (San Francisco, CA), Feb. 1978.
[12] Saleh, A. A. M., "Planar electrically symmetric N-way hybrid power dividers/combiners," *IEEE Trans. Microwave Theory Tech.*, vol. MTT-28, pp. 555–563, June 1980.
[13] R. Bellman, *Introduction to Matrix Analysis*. New York: McGraw-Hill, 1970, pp. 242–243.
[14] Peterson, D. F. and Haddad, G. I., "Design, performance and device/circuit limitations of N-way symmetrical IMPATT diode power combining arrays," Electron Physics Lab. Univ. Michigan, Ann Arbor, MI, Tech. Report AFWAL-TR-81-1107, Feb. 1981.

Dean F. Peterson (S'70–M'71) was born in Melbourne, FL, on March 28, 1945. He received the B.S. degree in electrical engineering from Utah State University, Logan, in 1967, and the M.S. and Ph.D. degrees from the Massachusetts Institute of Technology, Cambridge, in 1969 and 1971, respectively.

From 1971 to 1977 he was a staff member in the Satellite Communications Group at the Massachusetts Institute of Technology, Lincoln Laboratory, and was actively involved in the development of Lincoln Experimental Satellites (LES 8/9). He is currently an Assistant Professor in the Department of Electrical and Computer Engineering, Electron Physics Laboratory, The University of Michigan, Ann Arbor. His present research activities involve microwave solid-state devices and circuits.

Dr. Peterson is a member of Sigma Xi.

Tunable Low-Loss UHF Circulator for Cryogenic Applications

JARDA KADLEC

Abstract—**A 600-MHz above-resonance circulator operating at 4.2 K has been constructed and successfully tested. Its high isolation (>30 dB), extremely low insertion loss (<0.1 dB), low VSWR (<1.1), and acceptable instantaneous bandwidth (~6 percent) make it a promising device for utilization in narrow-band very low-noise systems.**

I. Introduction

THE NEED FOR low-loss cryogenic circulators had been recognized many years ago [1], [2]. In conjunction with low-noise reflection amplifiers, their importance follows from the consideration of noise contributions of preamplification losses to the system noise. This paper describes the design, construction, and performance of a Y-junction stripline circulator which is being used at the input of a low-noise superconducting unbiased parametric amplifier (SUPARAMP) operating at 4.2 K in a doubly-degenerate mode around 600 MHz [3], [4].

There are a number of publications [5] dealing with theory and design of stripline circulators for room temperature operation, most of them being more concerned with the broadbandness of the device than with minimization of its insertion loss. Only a few papers look into problems of low-temperature design of circulators operating in various frequency bands above 1 GHz [1], [2], [6]–[8]. To the author's knowledge, no work has been published on cryogenic circulators for frequencies below 1 GHz. We have constructed and tested two versions of a circulator designed for a nominal center-band frequency of 600 MHz. With regard to our anticipated application the minimum insertion loss has been emphasized at the expense of the

Manuscript received June 1, 1981; revised September 29, 1981. This work was supported in part by the National Science Foundation under Grant PHY-79-14602.

The author was with the Department of Physics and Astronomy, Louisiana State University, Baton Rouge, LA. He is now with the IBM Thomas J. Watson Research Center, P.O. Box 218, Yorktown Heights, NY 10598.

0018-9480/82/0200-0173$00.75 ©1982 IEEE